International Journal of Biological Macromolecules 249 (2023) 125957

Contents lists available at ScienceDirect

International Journal of Biological Macromolecules

journal homepage: www.elsevier.com/locate/ijbiomac

End-on PEGylation of heparin: Effect on anticoagulant activity and complexation with protamine

Sandra Amaral [a,b], Tamara Lozano-Fernández [c], Juan Sabin [d,e], Amanda Gallego [c], Alain da Silva Morais [a,b], Rui L. Reis [a,b], África González-Fernández [c,f,g], Iva Pashkuleva [a,b,*], Ramon Novoa-Carballal [a,b,*,1]

[a] 3B's Research Group, I3B's Research Institute on Biomaterials, Biodegradables and Biomimetics, University of Minho, Headquarters of the European Institute of Excellence on Tissue Engineering and Regenerative Medicine, 4805-017 Barco, Portugal
[b] ICVS/3B's – PT Government Associate Laboratory, University of Minho, Portugal
[c] NanoImmunoTech, Edificio CITEXVI Fonte das Abelleiras s/n, Campus Universitario de Vigo, 36310 Vigo, Pontevedra, Spain
[d] AFFINImeter Scientific & Development Team, Software 4 Science Developments, Santiago de Compostela, A Coruña 15782, Spain
[e] Departamento de Física Aplicada, Facultad de Física, Universidad de Santiago de Compostela, Santiago de Compostela, Spain
[f] CINBIO, Universidade de Vigo, Campus Universitario de Vigo, 36310 Vigo, Pontevedra, Spain
[g] Instituto de Investigación Sanitaria Galicia Sur (IIS-GS), Hospital Alvaro Cunqueiro, Estrada Clara Campoamor, 36312 Vigo, Pontevedra, Spain

ARTICLE INFO

Keywords:
Reducing end
Glycosaminoglycan
Oxime ligation
Protamine
Antithrombin
Isothermal calorimetry

ABSTRACT

Heparin is the most common anticoagulant used in clinical practice but shows some downsides such as short half-life (for the high molecular weight heparin) and secondary effects. On the other hand, its low molecular weight analogue cannot be neutralized with protamine, and therefore cannot be used in some treatments. To address these issues, we conjugated polyethylene glycol (PEG) to heparin reducing end (end-on) *via* oxime ligation and studied the interactions of the conjugate (Hep-*b*-PEG) with antithrombin III (AT) and protamine. Isothermal titration calorimetry showed that Hep-*b*-PEG maintains the affinity to AT. Dynamic light scattering demonstrated that the Hep-*b*-PEG formed colloidal stable nanocomplexes with protamine instead of large multi-molecular aggregates, associated with heparin side effects. The *in vitro* (human plasma) and *in vivo* experiments (Sprague Dawley rats) evidenced an extended half-life and higher anticoagulant activity of the conjugate when compared to unmodified heparin.

1. Introduction

High molecular weight heparin (HMWH) has been used clinically since 1935 to prevent coagulation related pathologies such as deep-vein thrombosis, pulmonary embolism, and thrombus in patients who suffered from a heart attack, stroke, or present atrial fibrillation. Despite an indisputable positive clinical outcome, HMWH has some downsides. It cannot be orally administrated and has a short therapeutic window. [1] It also triggers secondary effects, *e.g.* thrombocytopenia (low platelet count) in 1–5 % of patients, and osteoporosis in patients submitted to long-lasting heparin treatment. [2] Because of these drawbacks, HMWH is mainly used in clinical scenarios that require rapid neutralization of the anticoagulation effect (such as cardiac surgeries with cardiopulmonary bypass), in patients under renal failure and during haemodialysis. In these cases, protamine is the most common antidote used for neutralization. The protamine administration can induce three side effects: an anaphylactic reaction, hypotension, and pulmonary hypertension, which is problematic considering the common use of protamine in the clinics. Among these, the anaphylactic reaction occurs with an incidence of 0.19–0.69 % and has been related to the formation of specific IgG antibodies as well as to the formation of Hep/protamine aggregates, *i.e.*, multimolecular complexes. [3]

Some of the HMWH shortcomings have been addressed by its enzymatic or chemical depolymerization to low-molecular weight heparin (LMWH) also known as fractionated heparin. [1,4,5] LMWH has a prolonged therapeutic window and reduces, but does not eliminate, the risk

* Corresponding authors at: 3B's Research Group, I3Bs Research Institute on Biomaterials, Biodegradables and Biomimetics, University of Minho, Headquarters of the European Institute of Excellence on Tissue Engineering and Regenerative Medicine, 4805-017 Barco, Portugal.
E-mail addresses: pashkuleva@i3bs.uminho.pt (I. Pashkuleva), ramon.novoa@i3bs.uminho.pt (R. Novoa-Carballal).
[1] Current address: CINBIO, Universidade de Vigo, Campus Universitario de Vigo, 36,310, Vigo, Pontevedra, Spain.

https://doi.org/10.1016/j.ijbiomac.2023.125957
Received 29 May 2023; Received in revised form 20 June 2023; Accepted 15 July 2023
Available online 26 July 2023

of the heparin-induced thrombocytopenia type II and osteoporosis. [2,6] Additionally, only approximately 60 % of the LMWH activity can be neutralized, even with a big excess of protamine. This limitation is a consequence of the depolymerization process, which separates the sugar sequences that interact with protamine from those promoting anticoagulation. [6–10] Therefore, the same structural change that provides LMWH with a longer activity and controlled pharmacokinetics, turns difficult its neutralization and prevents its use under specific clinical circumstances. In these situations, HMWH is still being administered, despite the thrombocytopenia risk for the patient. A recent alternative to HMWH in the case of thrombo-prophylaxis related to cardiac surgeries is the use of direct oral anticoagulants (DOACs) and DOACs antidotes. [11] Currently, costly recombinant proteins are used as antidotes, although the clinical experience with them is limited, and the safety profile is still under debate. [12,13]

Homogenous, chemically or chemo-enzymatically derived ultra-low molecular weight heparins (ULMWH, M_n lower than 2 kDa) have also been described. [14] Among them, the specific pentasaccharide sequence that binds to antithrombin (AT) (Fondaxparin, Arixtra®) reached clinical use, but its high production cost is limiting its application. Moreover, the neutralization of ULMWH by protamine is similar to what it can be done with LMWH, *i.e.* it is not very efficient.

Herein, we investigated the possibility to prolong the activity of heparin without hampering its interaction with protamine by PEGylation at the reducing end. PEGylation is a well-known method to increase the half-life of proteins and drug delivery systems in blood. [15,16] Surprisingly, there is only one report on heparin PEGylation for anticoagulation purposes, where a non-selective modification (side-on) of LMWH is proposed. [17] From our point of view, the described methodology anticipates little applicability because the high exclusion volume of the PEG hinders the interaction of heparin with AT, preventing the subsequent inhibitory effect of thrombin and factor Xa (Fig. 1A). Thus, we propose an alternative chemo-selective end-on PEGylation of HMWH (Fig. 1B) to improve the pharmacodynamics of HMWH *in vivo* without compromising its anticoagulant effect and capacity of being neutralized by protamine.

2. Material and methods

2.1. Materials

Heparin sodium salt from porcine intestinal mucosa (Hep) was purchased from Sigma Aldrich (Grade I-A; 14 kDa; degree of sulfation determined by ^{1}H NMR, DS 1.8–2.4, 203 IU/mg). MeO-PEG-ONH_2 (5.2 kDa, determined by MALDI-TOF) was prepared through a two-step procedure from commercial MeO-PEG-OH as previously described. [19] Ultrafiltration membranes used for purification were obtained from Millipore (regenerated cellulose, Amicon ultra, MWCO 300 kDa). Phosphate buffer saline (PBS) was prepared from tablets (Sigma-Aldrich, 0.01 M phosphate buffer, 0.0027 M potassium chloride and 0.137 M sodium chloride, pH 7.4, at 25 °C) following the supplier instructions. HEPES and Antithrombin III (AT) were purchased from Sigma-Aldrich and NaCl from PanReac. Thromborel® S and Dade® Actin® FS reagents (Siemens Healthcare Diagnostics, Marburg, Germany) were used in the *in vitro* and *in vivo* assays to evaluate the prothrombin time (PT) and the activated partial thromboplastin clotting time (aPTT), respectively. Protamine (protamine sulfate for biochemistry, Merck) was used for the neutralization analysis.

2.2. Synthesis of end-on PEGylated heparin (Hep-b-PEG)

We have used a previously published procedure [20] with some modifications. Hep was dissolved in 0.5 % aq. AcOH (30 mg/mL, pH 3) and MeO-PEG-ONH_2 (5.2 kDa, 5 eq.) in DMSO (60 mg/mL). Equal volumes of both solutions were mixed and stirred at 45 °C for 24 h. The mixture was then added to an excess of water and freeze-dried. The obtained white foam was dissolved in water, and an excess of ethanol was added. The resulted opalescent solution was ultrafiltered against ethanol at 35 °C until the excess of MeO-PEG-ONH_2 was eliminated (confirmed by gel permeation chromatography, GPC). The product was then dissolved in water and freeze dried to yield a white foam. The purified Hep-*b*-PEG was characterized by GPC and ^{1}H NMR.

2.3. GPC analysis

GPC measurements were performed on a Malvern Viscotek TDA 305 with refractometer, right angle light scattering (RI detector 8110, Bischoff) and viscometer detectors. A set of four columns was used: precolumn Suprema, 5 μm, 8 × 50; Suprema 30 Å, 5 μm, 8 × 300; and 2× Suprema 1000 Å, 5 μm 8 × 300. The system was kept at 30 °C using PBS with 0.05 % *w/v* NaN_3 as eluent at a rate of 1 mL/min. The elution times of the RI detector signal were calibrated with a commercial polysaccharide set from Varian that contains 10 pullulans with narrow polydispersity and Mp (molecular mass at the peak maximum) ranging from 180 Da to 708 kDa. The molecular weight of Hep (14 kDa, PDI 1.28) was determined using the multidetector calibration mode on the Omnisec software.

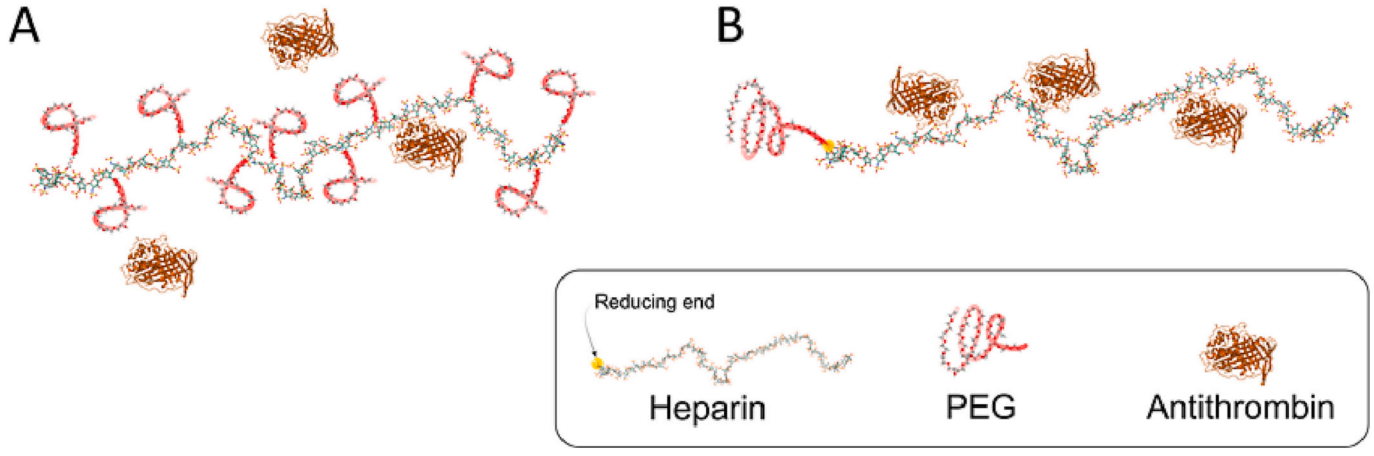

Fig. 1. Schematic representation of the difference between (A) side-on and (B) end-on PEGylation of heparin and its influence on the interactions with antithrombin: side-on PEGylation hampers the interaction with AT more significantly than end-on. The three-dimensional structures of heparin and AT II were downloaded from the Protein Data bank. The PEG is shown in mushroom conformation. [18].

2.4. NMR spectroscopy

^{1}H NMR spectra were recorded on a Bruker Avance 400 MHz spectrometer at 25 °C in D_2O. Chemical shifts are reported in ppm (δ units) downfield from 3-(trimethylsilyl)-propionic acid-d_4. The relaxation delay between pulses was set to 12 s to ensure that the ^{1}H NMR is quantitative. The signals of Hep were assigned according to previous works [21,22] and demonstrated the following composition for the used Hep: glucosamine residues: 71 % of GlcNS6S, 7 % of GlcNS, 3 % of GlcNS3S6S and 19 % of GlcNAc and uronic acid residues: 85 % of IdoA2S, 5 % of IdoA, 10 % of GlcA. The obtained Hep-*b*-PEG was analyzed at the same conditions. No differences were observed in the monosaccharide composition when compared to unmodified Hep.

^{1}H NMR of Hep-*b*-PEG (400 MHz, D_2O, 298 K): δ 5.57 (s, H1 of GlcNS6S linked to GlcA), 5.43–5.30 (m, H1 of GlcNS3S6S, GlcNS6S and GlcNS linked to IdoA2S), 5.20 (s, H1 of IdoA2S), 5.00 (s, H1 of IdoA), 4.82 (s, H5 of IdoA2S), 4.42 (d, $J = 11.7$ Hz, H6 of GlcNS6S), 4.34 (s, H2 of IdoA2S), 4.25–3.95 (m, H6 and H5 of GlcN6S + H3 and H4 of IdoA2S), 3.90–3.60 (m, H3, H4 of GlcNS6S and CH_2O of PEG), 3.49–3.35 (m of protons of GlcA, GlcNS6S linked to GlcA and GlcNS3S6S and CH_3O of PEG), 3.28 (d, $J = 11.2$ Hz, H2 of GlcNS6S), 2.04 (br s, *N*-acetylmethyl protons of GlcNAc).

To determine the degree of PEGylation, the signals between 3.45 and 4.56 (heparin plus CH_2O of PEG) were integrated *versus* the *N*-acetylmethyl protons of GlcNAc and compared to the ratio of those signals before PEGylation in the spectrum of unmodified Hep. The number of repeating units of PEG, necessary to calculate the degree of PEGylation was determined from the Mn, 5241 kDa measured previously by MALDI-TOF. [23] The degree of PEGylation was determined to be 98.5 %, *i.e.*, the reaction is nearly quantitative as observed for other polysaccharides. [20,23,24]

2.5. Dynamic light scattering (DLS)

Solutions of protamine, Hep and Hep-*b*-PEG were prepared in PBS and filtered (220 nm) before the DLS titration. Protamine is a mixture of peptides whose precise composition is not provided by the supplier. Therefore the heparin/protamine ratios are expressed in mass as previously described. [25] The titration was performed manually. Of note, the solutions were not filtered after each subsequent addition due to the anticipated flocculation. Two sets of experiments were performed: (i) the addition of protamine over Hep or Hep-*b*-PEG and (ii) the addition of Hep or Hep-*b*-PEG over protamine. Hep/protamine mass ratios were analyzed in the range 93–0.05, always using the same molar concentration for Hep and Hep-*b*-PEG. As an example, protamine 1.83 g/L was added to 280 μL of Hep (0.6 g/L, 0.05 mM) or 280 μL of Hep-*b*-PEG (0.84 g/L, 0.05 mM) in the DLS cell. The titrations were performed with *ca.* 15–19 subsequent additions (5, 50 or 100 μL of titrant) and the size of the complexes was analyzed on a Malvern NanoZS instrument with a He—Ne laser after *ca.* 2 min of each addition. Size measurements were performed at an angle of 173° at room temperature. The average hydrodynamic radius (Rh) and polydispersity index (PDI) were determined by fitting the correlation function with the cumulant method. The size was measured 3 times in the DLS equipment after each addition, and 3–4 independent experiments were performed to confirm the reproducibility of the results.

2.6. Isothermal titration calorimetry (ITC)

ITC was carried out with a MicroCal PEAQ-ITC instrument. The reference cell was loaded with Milli-Q water. The feedback/gain mode was set to high. A typical experiment involved an initial injection of the titrant (0.25 to 1 μL) followed by a series of 20–40 injections of the same solution (1 or 2 μL) with an interval of 120 s between injections. Hep (6 g/L, 0.5 mM) or Hep-*b*-PEG (8.6 g/L, 0.5 mM) were used as a titrant over a solution of antithrombin (AT, 0.68 g/L, 11 μM) that was loaded inside the cell. All solutions were prepared in Hepes buffer (10 mM, pH 7.4, 150 mM NaCl). The sample in the cell was stirred at 750 rpm and the experimental temperature was maintained at 25 °C. Control titration experiments of Hep over the HEPES buffer and the HEPES buffer over AT at each specific AT or Hep concentration demonstrated negligible dilution heat as compared to the heat of interaction. Experiments under similar conditions but with Hep or Hep-*b*-PEG previously complexed with protamine (6 mg/mL, in a 1.3 mass ratio) were performed to investigate the interaction of neutralized Hep with AT. At least 3 independent experiments were performed per each condition.

MicroCal PEAQ-ITC Analysis Software and AFFINImeter Software were used for data analysis. The area under each peak of the resulting heat profile was integrated, normalized by the concentrations, and plotted against the molar ratio of the ligand to the protein. The resulting binding isotherms were fitted by nonlinear regression using a one set of sites model and two sets for sites with the MicroCal software. The stoichiometry of the interaction (n), the equilibrium dissociation constant (K_D), and the change in enthalpy (ΔH) were obtained from the fitting of all titration data. The change of Gibbs free energy (ΔG) was calculated from Eq. (1) and the change of the entropy (ΔS) was obtained from Eq. (2),

$$\Delta G = RT \ln K_D \quad (1)$$

$$\Delta G = \Delta H - T\Delta S \quad (2)$$

where R is the gas constant and T the temperature.

AFFINImeter software was used to apply a competitive model for the Hep/AT interaction as previously described. [26,27] This model assumes that Hep contains pentasaccharide regions with a high AT affinity and a group of low-affinity regions with non-specific binding (Eq. (3)). The amount of pentasaccharide was, *a priori*, unknown and was used as a fitting parameter in the model, assuming that the molar sum of high and low affinity regions was fixed to the nominal total Hep concentration.

$$AT - Hep_{high} \leftrightarrow AT + Hep \leftrightarrow AT - Hep_{low} \; [Hep] = [Hep]_{low} + [Hep]_{high} \quad (3)$$

The relative molar concentration of high and low-affinity regions, and independent affinity and thermodynamic parameters (ΔH, ΔS, ΔG) were determined. Global fitting of two separate ITC experiments was performed to the experimental data to avoid over-parameterization of the analysis.

2.7. Coagulation times (in vitro)

Human peripheral venous blood was obtained from volunteers using sodium citrate as anticoagulant. A pool of plasma from at least three human healthy donors was used within 8 h after collection.

Stock solutions of MeO-PEG-ONH_2, Hep-*b*-PEG and HMWH were diluted in PBS to concentrations corresponding to 50, 25, 10 and 5 IU/mL. The Hep concentration was converted to Hep units using the manufacturer instructions. In the case of Hep-*b*-PEG, the conversion was based on the Hep content determined by NMR and assuming that Hep activity was not modified by the presence of PEG. Considering 98.5 % of conversion (NMR), Mn of 14 kDa for Hep (GPC-MALS), and Mn of 5.2 kDa for PEG (MALDI-TOF), a mass percentage of 73 % Hep in Hep-*b*-PEG was calculated.

The tubes containing plasma and polymers were incubated for 15, 30 or 60 min at 37 °C. Plasma incubated only with PBS was used as control. After this incubation, a STart 4 coagulometer from Diagnostica Stago, (Parsippany, NJ, USA) was used to measure the different coagulation times (PT, aPTT and TT). The reagents needed to induce the coagulation cascade were added to the treated plasma, while the solution was magnetically stirred. The time between the addition of the reagents until the formation of the clot was automatically determined by the equipment. Each coagulation time was measured 3 times.

2.8. Coagulation times (in vivo)

2.8.1. Animal experimentation

The maintenance and use of animals were carried out in accordance with the Ethics Committee of University of Minho and approved by the Portuguese Licensing Authority (Direcção Geral de Alimentação e Veterinária, DGAV) under the authorized project number 008071. Male Sprague Dawley rats (32 rats *ca.* 330 g, Charles River, USA) were divided in 5 groups according to the administered doses (100, 200, 300 and 600 IU/Kg, and PBS as control) for normal coagulation times. The maximum volume of the solutions injected at the tail vein was lower than 0.3 mL (Hep or Hep-*b*-PEG solutions from 1 to 6 mg/mL). The tail of the rat was first disinfected with ethanol 70 % and the samples were injected using a 25G needle. At specific time points (15, 30, 60, 120 and 180 min) the rats were anesthetized through intra-peritoneal injection of a mixture of Ketamin (75 mg/Kg) and Medetomidin (0.5 mg/Kg). The blood samples (3 mL) were collected through cardiac puncture, using an 18G needle and sterile (EDTA) anticoagulated tubes. Then, the animals were sacrificed by intracardiac injection of pentobarbital sodium overdose (200 mg/Kg). The blood collected was centrifuged at 3000 rpm for 10 min, and the plasma was recovered for evaluation of the aPTT and the PT.

2.8.2. PT and aPTT assessment

Plasma from rat blood samples collected at different time points were incubated for 1 min at 37 °C. The PT and aPTT were determined using a Siemens CA540 coagulometer, by following the manufacturer's protocols (Siemens Healthcare Diagnostics, Marburg, Germany). Each coagulation time was measured 3 times.

3. Results and discussion

3.1. Synthesis of Hep-b-PEG

The modification of proteins and peptides with PEG is a well-established approach for an extension of the therapeutic window of these biomolecules, and there is a large body of evidences showing that the position of PEG is crucial for the bioactivity of the conjugate. [28] We have previously developed a simple method for end-on PEGylation of glycosaminoglycans (GAGs), which comprises oxime click reaction between an aminooxy terminated PEG and the reducing end of Hep (Fig. 2A). [20,23,24] The selectivity of this method is due to the aminooxy group at the PEG end that reacts only with GAG reducing end. The obtained conjugates are cytocompatible and biofunctional as demonstrated by their interaction with basic fibroblast growth factor (FGF-2). [20] Herein, we applied similar synthetic approach but the removal of the PEG excess was performed by ultrafiltration instead of dialysis - a change that brings benefits in terms of time, scalability, and sustainability, given the reusability of the membrane, and the less volume of solvent required. The new purification procedure resulted in a high purity product (confirmed by GPC), validating the successful

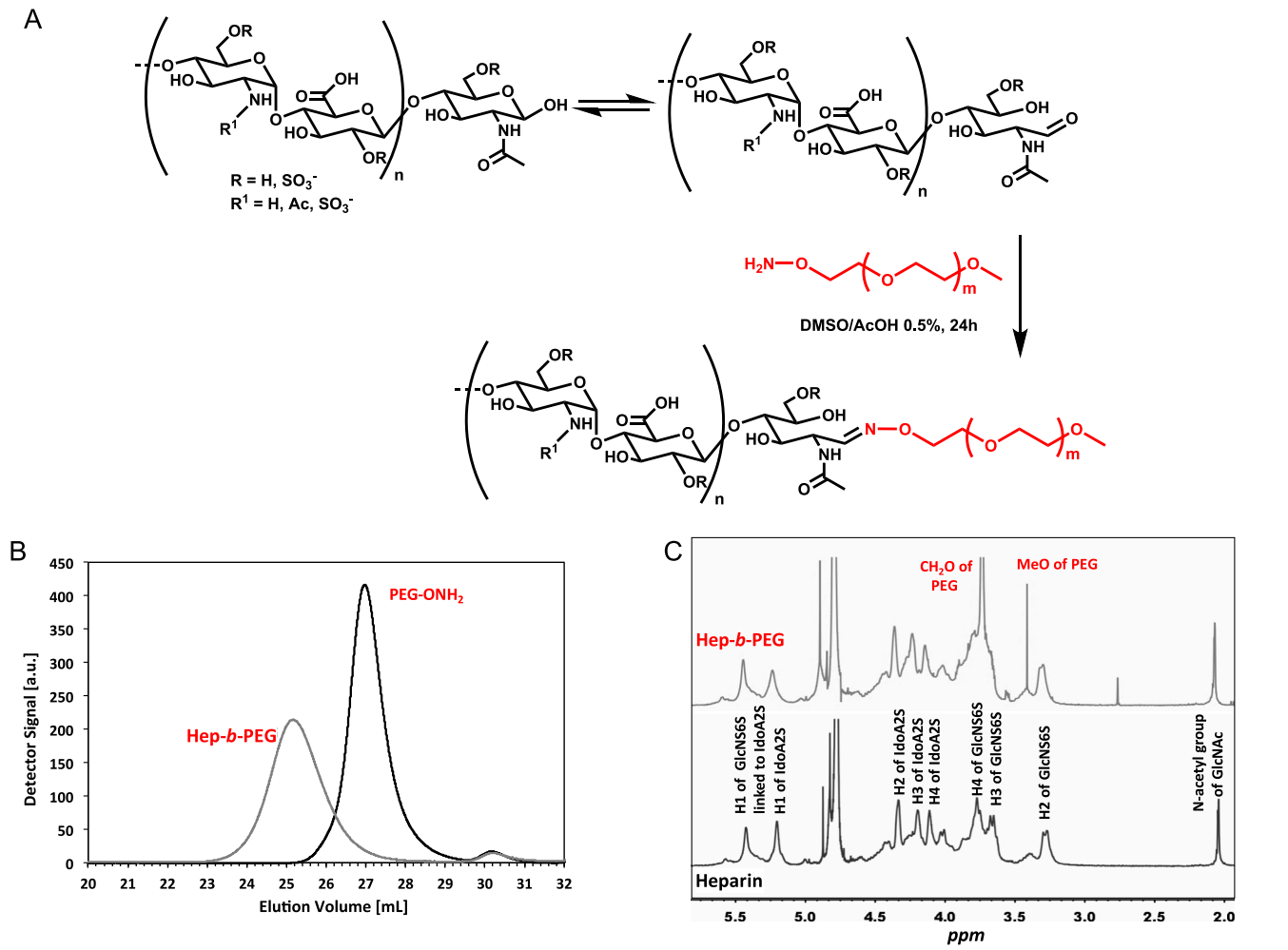

Fig. 2. (A) Schematic presentation of the oxime click reaction used for the synthesis of Hep-*b*-PEG. (B) The purity of the obtained product was confirmed by GPC, and (C) its structure was validated by ^{1}H NMR according to previous data [22]; [21]. In the ^{1}H NMR of heparin only the major signals (saccharides at high proportion) are labelled.

conjugation and purification (Fig. 2B). The structure of the PEG-*b*-Hep was analyzed by ^{1}H NMR spectroscopy (Fig. 2C) - the oxime peak is not visible in the spectrum (this peak is usually absent in the spectra of high molecular weight polysaccharides such as dextran, chitosan, hyaluronan [29–31]) but the peak corresponding to the CH_2O- of the PEG is visible at 3.7 ppm while free PEG is missing from the GPC elugram, confirming the successful conjugation. The integration of the CH_2O- signal *versus* the acetyl group of Hep was used to determine the PEGylation degree as detailed in the materials and methods section and showed that the end-on modification is nearly quantitative (98.5 %). The stability of the formed oxime bond was assessed by GPC: we did not observe any hydrolysis (free PEG) along the studied 2 weeks.

3.2. Interaction of Hep and Hep-b-PEG with antithrombin (AT)

The preservation of the anticoagulant properties after PEGylation is imperative for the proposed application. Isothermal titration calorimetry (ITC) was used to study the effect of the end-on PEGylation of Hep on its binding affinity to AT *in vitro*. This technique allows the determination of the affinity constant and all thermodynamic parameters (ΔH, ΔG, and ΔS) of the binding in a single titration experiment. ITC titration was performed by adding Hep or Hep-*b*-PEG into a solution of AT. The data were initially fitted with MicroCal Software to the simplest model that assumes one binding site on Hep or Hep-*b*-PEG. Using this model, we obtained similar affinities $K_{D[Hep]} = (1.7 \pm 0.5)\ x\ 10^{-6}$ M and $K_{D[Hep\text{-}b\text{-}PEG]} = (1.2 \pm 0.3)\ x\ 10^{-6}$ M, and stoichiometry close to 2 (for Hep or Hep-*b*-PEG 0.5 mM and AT 11 μM) for both molecules. Nevertheless, isotherms clearly show two different slopes before reaching saturation. A closer look at the thermograms reveals that each heat peak is constituted by two separate signals (Fig. 3A and B), indicating a complex binding process that requires a specific model. AT interacts specifically with Hep *via* a pentasaccharide sequence to which binds with high affinity and by additional non-specific weak supramolecular interactions. [32] A previous study of Hep/AT interaction by ITC has used a competitive model between the low and high affinity regions of Hep for AT (Eq. (1)). [27] Indeed, the application of this model to our experimental data using AFFINImeter software revealed a better fitting of the experimental data (Fig. 3C and D) and provides information for the thermodynamic parameters of the interactions (Table 1) and for the molar ratio of pentasaccharide in Hep and Hep-*b*-PEG. At the beginning of the titration, AT is in excess and binds to all regions (pentasaccharide

Table 1
Thermodynamic parameters for the interaction of AT with the low and high affinity regions of Hep and Hep-*b*-PEG. Data are presented as average values ± standard deviation.

	Region	% molar	K_D [M]	ΔH [cal/mol]	TΔS (cal/mol)	ΔG (cal/mol)
Hep	Low	62.2 ± 0.1	$(3.0 \pm 1.0) \times 10^{-5}$	$(-8.0 \pm 3.0) \times 10^{3}$	-5.3×10^{3}	-2.7×10^{3}
	High	37.7 ± 0.1	$(6.0 \pm 1.0) \times 10^{-8}$	$(-1.3 \pm 0.1) \times 10^{4}$	-8.7×10^{4}	-4.3×10^{3}
Hep-*b*-PEG	Low	57.1 ± 0.1	$(3.8 \pm 0.1) \times 10^{-5}$	$(-1.2 \pm 0.1) \times 10^{4}$	-9.3×10^{3}	-2.7×10^{3}
	High	42.9 ± 0.1	$(1.3 \pm 0.1) \times 10^{-7}$	$(-2.0 \pm 1.0) \times 10^{4}$	-1.6×10^{4}	-4.1×10^{3}

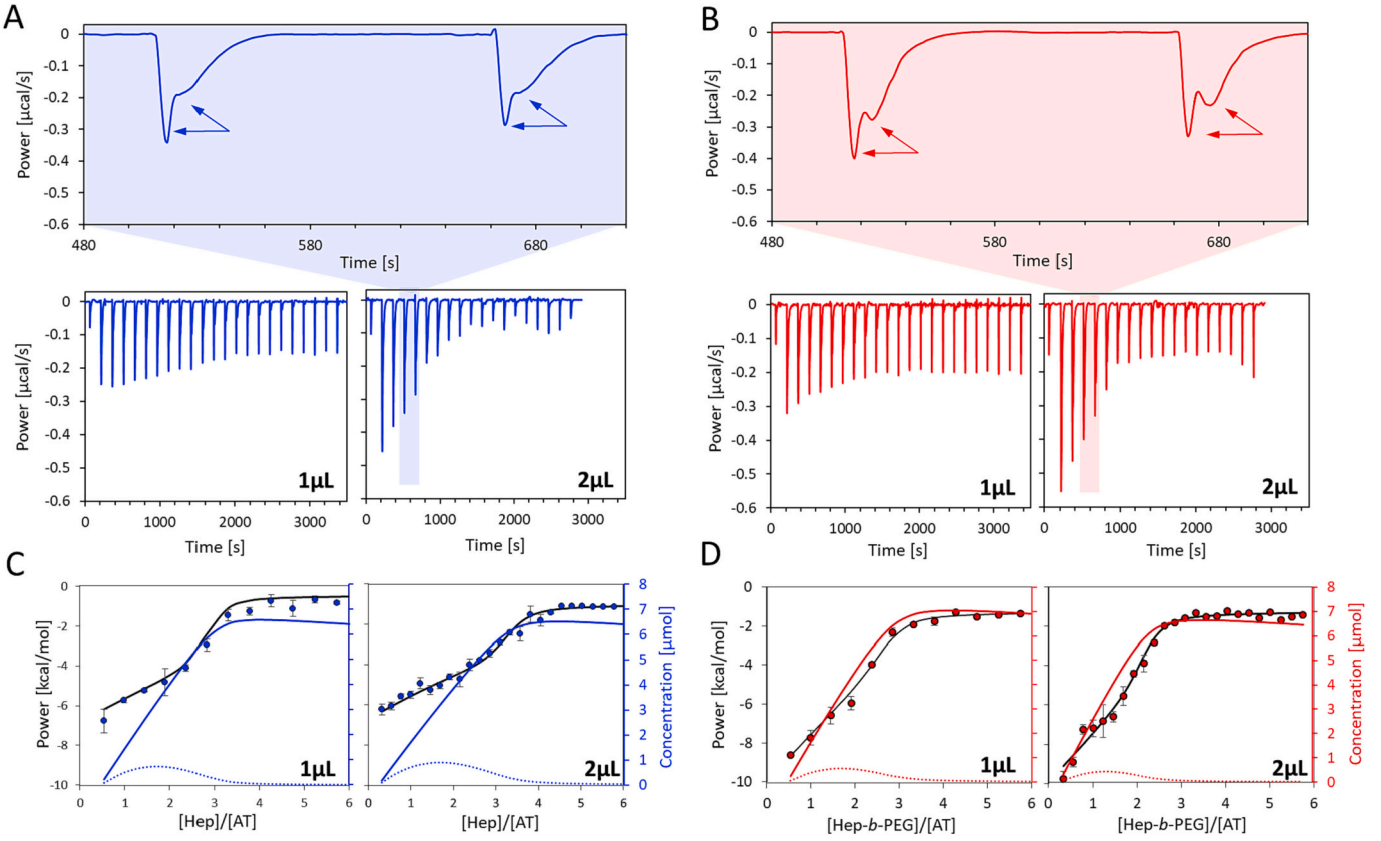

Fig. 3. ITC analysis of AT interactions with Hep and Hep-*b*-PEG. Representative thermograms of the titration of AT with (A) Hep (blue) and (B) Hep-*b*-PEG (red). Expansion of the ITC thermograms shows two separate heat events after each injection. Isotherm points (filled bullets) and global fitting analysis (black lines) of the data for (C) Hep/AT and (D) Hep-*b*-PEG/AT applying a competitive model; dashed lines show the variation of the concentration of complexes of AT with low affinity regions and the solid coloured (blue or red) lines represent the concentration of complexes of AT with high affinity regions.

and low affinity regions) of Hep and Hep-*b*-PEG. As the titration progresses, the relative concentration of AT in the system decreases, and it binds only to the high affinity pentasaccharide regions.

The thermodynamic data demonstrated that the PEGylation did not significantly affect the interaction with AT as similar parameters and relative concentrations of high affinity regions were obtained for Hep and Hep-*b*-PEG (Table 1). A small decrease in the affinity of Hep-*b*-PEG to the pentasaccharide regions of AT was observed and although this finding agrees with our hypothesis (Fig. 1A), the difference in the K_D values is not significant to make a conclusion only from these data, especially considering that the binding affinities with the pentasaccharide are quite high, near the detection limit of the calorimeter. When AT was added to a protamine/Hep-*b*-PEG complex (formed at a mass ratio of 1.3), we did not observe any interaction between AT and Hep-*b*-PEG (Fig. S1), showing an efficient inhibition of Hep-*b*-PEG by protamine.

3.3. Interaction of Hep-b-PEG and Hep with protamine

Hep and protamine form a strong, neutral polyelectrolyte complex that isolates Hep from AT II, *i.e.* neutralizes Hep. [3] The complexation is based on electrostatic interactions and thus, it is mechanistically similar to the process that initiates the heparin-induced thrombocytopenia (HIT). [25]

Previous studies have used turbidity and dynamic light scattering (DLS) to determine the quantity of protamine needed for Hep flocculation (*i.e.*, precipitation of colloidal particles). These studies report a ratio of protamine/Hep = 1.4 as optimal and highlight the advantages of DLS in terms of sensitivity. [3] Herein, we used DLS and performed titrations of protamine over Hep and Hep-*b*-PEG, covering a wide range of mass ratios (Figs. 4 and S2).

Complexation for both polymers was observed but they behaved differently. In an absence of protamine, Hep and Hep-*b*-PEG have hydrodynamic radius of 20–24 nm and large polydispersity index (PDI 0.7–0.9) as expected for a polyelectrolyte in solution. Upon addition of protamine, Hep and Hep-*b*-PEG formed nanocomplexes (hydrodynamic radius of protamine/Hep complex was about 80 nm and protamine/Hep-*b*-PEG complex was about 30 nm and small PDIs of 0.2). Protamine/Hep complexes grew from nano to the micrometre size upon increasing the mass ratio, but the protamine/Hep-*b*-PEG complexes remained small, *i.e.* about 30 nm for all tested ratios (Fig. 4A), indicating formation of homogenous complexes stabilized by PEG induced a stealth effect (Fig. 5). [24,33]

The significant increase of the radius observed for protamine/Hep was confirmed by the visible turbidity at mass ratio ≥ 1, whilst in the case of protamine/Hep-*b*-PEG (small size of the complexes) no turbidity occurred. The count rate (related to the complex concentration) revealed more differences between the systems (Fig. 4B). For protamine/Hep-*b*-PEG complexes, the maximum count rate reached a plateau at a mass ratio of 1.8, whilst in the case of the protamine/Hep system, a maximum count rate was observed at a mass ratio of 1, and the addition of more protamine resulted in a count rate decrease. This decrease is most probably due to the observed precipitation (turbidity) and was accompanied by a significant polydispersity (Fig. 4C) [35]: the PDI steeply increased for protamine/Hep, but remained at low values (under 0.08) for protamine/Hep-*b*-PEG. We also performed an experiment in which a titration of Hep or Hep-*b*-PEG over protamine was done (Fig. S2). This experiment mimics the clinical scenario, in which protamine is injected (*i.e.* concentrated) in the bloodstream and gives information about the aggregation immediately upon injection. In this experimental setup, protamine/Hep formed less disperse complexes (lower precipitation), and the results with Hep-*b*-PEG were similar to the

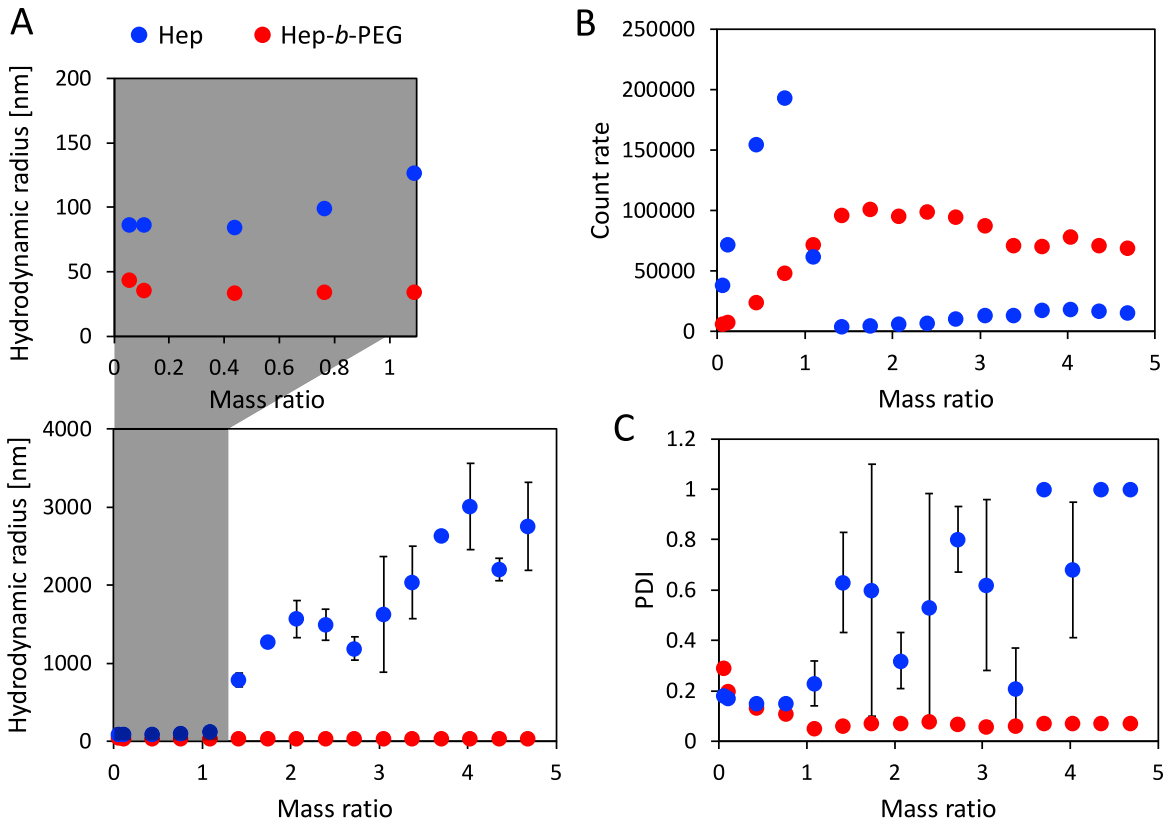

Fig. 4. DLS data showing the complexation of Hep and Hep-*b*-PEG upon addition of protamine at different mass ratios (expressed as protamine/Hep): Change of (A) hydrodynamic radius (the upper graph is expansion of the region 0–1 of mass ratio), (B) count rate and (C) polydispersity index (PDI) in a function of the ratio between protamine and Hep (blue) or Hep-*b*-PEG (red). Data are presented as average values and standard deviations for $n = 3$. Of note, error bars are shown for all data but not visible when they are smaller than the symbol.

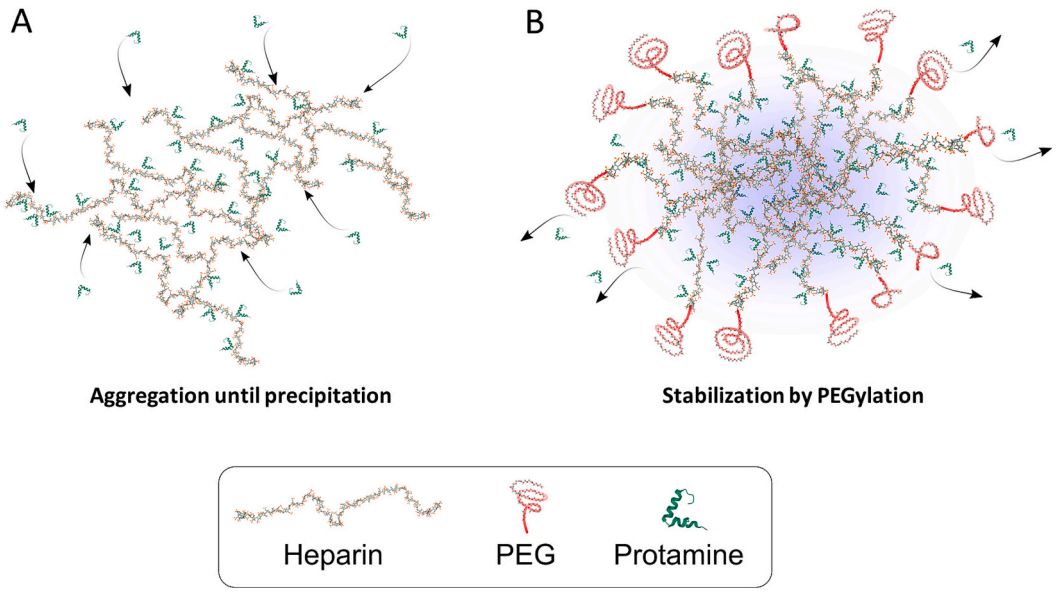

Fig. 5. Schematic presentation of different mechanisms of complexation of protamine with Hep and Hep-*b*-PEG as suggested by the DLS data: (A) protamine/Hep complexes can grow in all directions, while (B) the growth of protamine/Hep-*b*-PEG is constraint by the stealth effect induced *via* the PEGylation. The three-dimensional structures of Hep was downloaded from the Protein Data bank. The conformation of protamine was obtained using the software I-TASSER as previously reported. [34].

reported in Fig. 4, evidencing assembly of the same type of small and stable complexes despite the different stoichiometry.

Of note, the titration experiments were performed at physiological ionic strength and are thus indicative for the clinical outcome. The results anticipate that either Hep or Hep-*b*-PEG can be neutralized by protamine and that the PEGylation might reduce HIT that is triggered by the formation of multi-molecular complexes [2]. The occurrence of HIT has also been associated with the administration of protamine, following a similar mechanism that might also be alleviated by the end-on PEGylation of Hep. [25]

3.4. *In vitro activity of Hep-b-PEG*

Plasma from human donors was used to investigate the anticoagulant properties of Hep-*b*-PEG *in vitro*. Controls with PBS and PEG discarded the potential influence of the PEG alone in the coagulation process. Similar PT, aPTT and TT values for Hep and Hep-*b*-PEG were obtained at a concentration of 50 IU (Table S1). Experiments at a lower dose (25, 10 IU) and different incubation times (15, 30 and 60 min) also showed similar behaviour for Hep and Hep-*b*-PEG (Fig. 6, Table S1). However, the PT at a concentration of 5 IU clearly shows a higher activity of the Hep-*b*-PEG when compared with Hep (108.0 *vs* 12.7, respectively, for 60 min of incubation). This result might be attributed to the steric hindrance provided by the PEG, which reduces the interaction of Hep with other proteins in the blood plasma.

3.5. *In vivo activity of Hep-b-PEG*

The *in vitro* results, showing the preservation of the anticoagulant properties of the Hep-*b*-PEG, were further confirmed by an *in vivo* assay in Sprague Dawley rats (Fig. 7).

Hep-*b*-PEG presented equal (for the highest dose) or longer

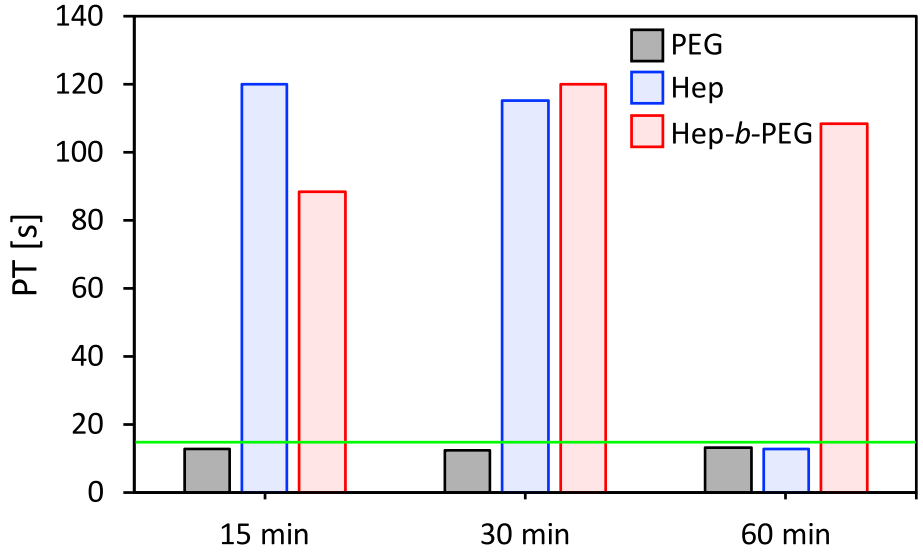

Fig. 6. PT using human plasma in the presence of Hep (blue), Hep-*b*-PEG (red) and PEG (grey) at a concentration of 5 IU. Green line marks the level of the normal coagulation times (PBS control, Table S1), measured in seconds.

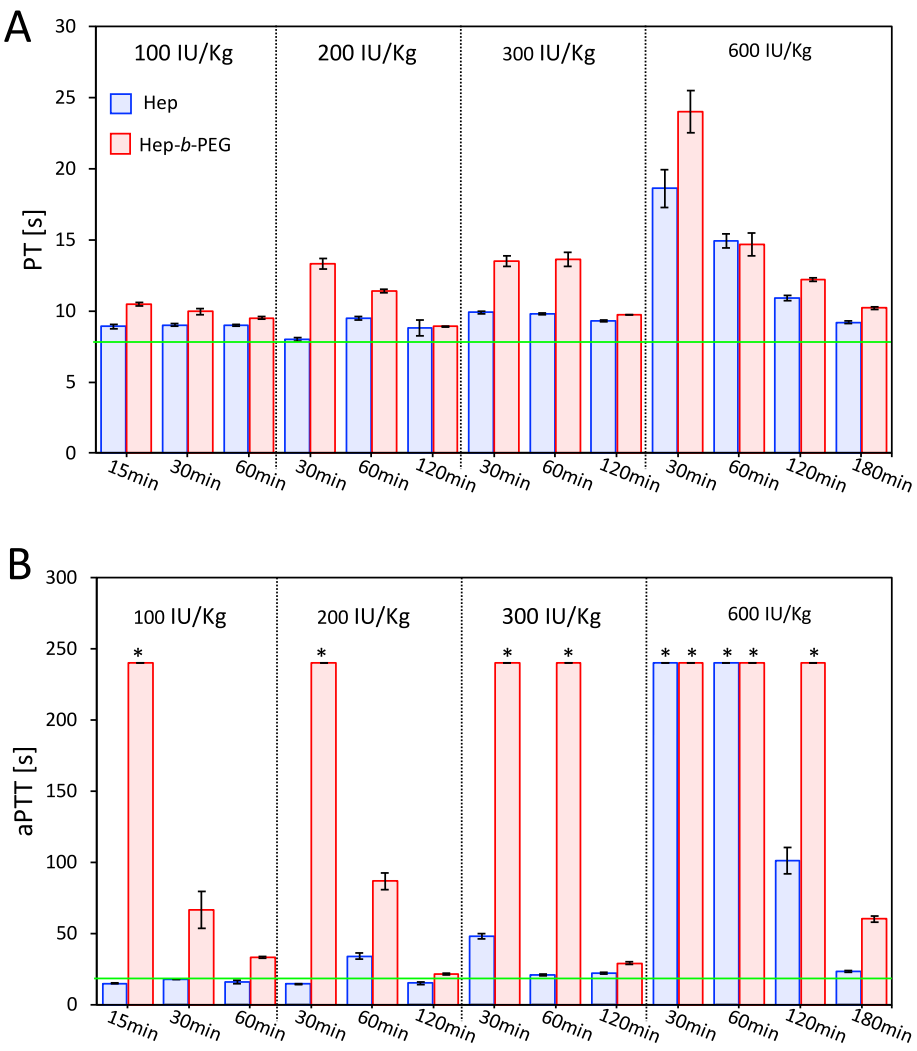

Fig. 7. Coagulation properties after *in vivo* administration. (A) PT and (B) aPTT times (measured in seconds) were tested in plasma from rats treated with different concentrations of Hep (blue) and Hep-*b*-PEG (red). *Values of aPTT were determined until 240 s and the marked bars correspond to times equal or longer than 240 s. The green line marks the level of the normal coagulation times observed upon injection of PBS as control. Data are presented as average values with the respective standard deviation for $n = 3$.

coagulation times than Hep for all studied concentrations and time points (Fig. 7). A closer look to the aPTT at lower concentrations revealed that a low dose of Hep does not change significantly the coagulation times, while Hep-*b*-PEG increased aPTT significantly (*e.g.* 15 min and 30 min for 100 and 200 IU/Kg). Of note, aPTT time is used in clinical practice to adjust the dose of Hep and monitor its effect. This is because aPTT is sensitive to the inhibitory effects of Hep on thrombin, factor Xa, and factor IXa. [36]. Additional experiments showed that after 2, 3 and 6 h, animals treated with Hep-*b*-PEG at 100, 200, 300 IU/kg present normal PT and aPTT as previously reported in the literature for Hep. [1]. The increase of the aPTT (but not of the PT) for unmodified heparin is smaller than the previously reported values obtained using the same animal model [37], which can be due to the use of different Hep and/or APTT reagents. In any case, herein we have used and compared the same Hep batch, PEGylated or not, to avoid any bias due to different Hep activity.

These results show that the end-on PEGylation affects the clearance of the Hep-*b*-PEG. Hep is eliminated from the bloodstream through a complex mechanism: a rapid saturable phase activated *via* Hep binding to endothelial cells and macrophages, and a slower phase that follows a first-order non-saturable mechanism, being primarily renal. [1,4,7,36] Our data suggest that PEGylation of Hep moderates unspecific interactions with plasma proteins (as described for numerous proteins and drug delivery systems [38], endothelial cells and macrophages, all of them related to the saturable phase of clearance, thus changing the pharmacodynamics of Hep-*b*-PEG.

4. Conclusions and outlook

The end-on PEGylation of Hep prolongs and enhances its anticoagulant effect at low doses. When compared to LMWH, Hep-*b*-PEG has the benefits of interacting with protamine and avoid the formation of large multi-molecular complexes associated with Hep side effects. These features can have advantages in clinical applications, which require neutralization with protamine after the therapy. Moreover, the increased activity observed for Hep-*b*-PEG implies that a lower dose can be used compared to the unmodified Hep in a surgical scenario, which will be beneficial in terms of minimizing the potential secondary side effects.

CRediT authorship contribution statement

S.A. and R.N.-C.: polymer synthesis and characterization; S.A., R.N·C and J.S.: ITC experiments; R.N.C., T.L and A.G.: coagulation times; R.NC and R.N.-C. and I.P.: concept and planning; S.A. and R.N.C., writing original draft manuscript; R.N.C., I.P. A.G. F., J.S, writing - Review & Editing; R.L.R., I.P., R.N.-C., A.G.R: supervision and funding; all authors read, corrected, and approved the manuscript.

Declaration of competing interest

The authors declare that they have no known competing financial interests or personal relationships that could have appeared to influence

the work reported in this paper.

The authors declare the following financial interests/personal relationships which may be considered as potential competing interests: Sandra Amaral, Tamara Lozano-Fernández, Juan Sabin, Amanda Gallego, Alain da Silva Morais, Rui L. Reis, África González-Fernández.

Acknowledgements

The authors thank INNO Laboratório Veterinário for the measurements of *in vivo* coagulation times, Raul Pacheco for discussions about the ITC results, Teresa Oliveira for her help in the *in vivo* experiments and Ramón Rail for his help in the 3D structures of Figs. 1 and 4. We thank funding provided by the Portuguese Foundation for Science and Technology (PTDC/QUI-POL/28117/2017 and CEECIND/00814/2017). África González-Fernández thanks Xunta de Galicia (Grupo de Referencia competitiva, GRC-ED431C 2020/02) 2020-2023.

Appendix A. Supplementary data

Supplementary data to this article can be found online at https://doi.org/10.1016/j.ijbiomac.2023.125957.

References

[1] B. Boneu, C. Caranobe, P. Sie, 3 pharmacokinetics of heparin and low molecular weight heparin, Baillière's Clinical Haematology 3 (3) (1990) 531–544.
[2] I. Ahmed, A. Majeed, R. Powell, Heparin induced thrombocytopenia: diagnosis and management update, Postgrad. Med. J. 83 (983) (2007) 575–582.
[3] E. Sokolowska, B. Kalaska, J. Miklosz, A. Mogielnicki, The toxicology of heparin reversal with protamine: past, present and future, Expert Opin. Drug Metab. Toxicol. 12 (8) (2016) 897–909.
[4] G.J. Merli, J.B. Groce, Pharmacological and clinical differences between low-molecular-weight heparins: implications for prescribing practice and therapeutic interchange, P T 35 (2) (2010) 95–105.
[5] L. Zhu, M. Li, Y. Liu, Intravenous administration of low-molecular-weight heparin, Am. J. Ther. 26 (3) (2019) 426–428.
[6] G.R. Hetzel, C. Sucker, The heparins: all a nephrologist should know, Nephrology Dialysis Transplantation 20 (10) (2005) 2036–2042.
[7] J. Hirsh, T.E. Warkentin, S.G. Shaughnessy, S.S. Anand, J.L. Halperin, R. Raschke, C. Granger, E.M. Ohman, J.E. Dalen, Heparin and low-molecular-weight heparin mechanisms of action, pharmacokinetics, dosing, monitoring, efficacy, and safety, CHEST 119 (1) (2001) 64S–94S.
[8] E.I. Oduah, R.J. Linhardt, S.T. Sharfstein, Heparin: past, present, and future, Pharmaceuticals 9 (3) (2016) 38–50.
[9] M. Schroeder, J. Hogwood, E. Gray, B. Mulloy, A.-M. Hackett, K.B. Johansen, Protamine neutralisation of low molecular weight heparins and their oligosaccharide components, Anal. Bioanal. Chem. 399 (2) (2011) 763–771.
[10] M.A. Crowther, L.R. Berry, P.T. Monagle, A.K.C. Chan, Mechanisms responsible for the failure of protamine to inactivate low-molecular-weight heparin, Br. J. Haematol. 116 (1) (2002) 178–186.
[11] J.H. Levy, J.M. Connors, Andexanet alfa use in cardiac surgical patients: a Xa inhibitor and heparin reversal agent, J. Cardiothorac. Vasc. Anesth. 35 (1) (2021) 265–266.
[12] G. Erdoes, C. Reid, A. Koster, Oral anticoagulants in cardiovascular surgery: between nightmare tour and safe cruise, J. Cardiothorac. Vasc. Anesth. 33 (2) (2019) 302–303.
[13] A. Greinacher, T. Thiele, K. Selleng, Reversal of anticoagulants: an overview of current developments, Thromb. Haemost. 113 (05) (2015) 931–942.
[14] M. Qiao, L. Lin, K. Xia, J. Li, X. Zhang, R.J. Linhardt, Recent advances in biotechnology for heparin and heparan sulfate analysis, Talanta 219 (2020), 121270.
[15] C. Monfardini, F.M. Veronese, Stabilization of substances in circulation, Bioconjug. Chem. 9 (4) (1998) 418–450.
[16] R. Duncan, M.J. Vicent, Polymer therapeutics-prospects for 21st century: the end of the beginning, Adv. Drug Deliv. Rev. 65 (1) (2013) 60–70.
[17] A.K. Choubey, C.P. Dora, T.D. Bhatt, M.S. Gill, S. Suresh, Development and evaluation of PEGylated enoxaparin: a novel approach for enhanced anti-Xa activity, Bioorg. Chem. 54 (2014) 1–6.
[18] C. Cruje, D.B. Chithrani, Polyethylene glycol functionalized nanoparticles for improved cancer treatment, Reviews in Nanoscience and Nanotechnology 3 (1) (2014) 20–30.
[19] T.L. Schlick, Z. Ding, E.W. Kovacs, M.B. Francis, Dual-surface modification of the tobacco mosaic virus, J. Am. Chem. Soc. 127 (11) (2005) 3718–3723.
[20] C. Silva, A. Carretero, D. Soares da Costa, R.L. Reis, R. Novoa-Carballal, I. Pashkuleva, Design of protein delivery systems by mimicking extracellular mechanisms for protection of growth factors, Acta Biomater. 63 (2017) 283–293.
[21] T. Toida, Y. Huang, Y. Washio, T. Maruyama, H. Toyoda, T. Imanari, R.J. Linhardt, Chemical microdetermination of heparin in plasma, Anal. Biochem. 251 (2) (1997) 219–226.
[22] X. Zhang, V. Pagadala, Hannah M. Jester, A.M. Lim, T.Q. Pham, A.M.P. Goulas, J. Liu, R.J. Linhardt, Chemoenzymatic synthesis of heparan sulfate and heparin oligosaccharides and NMR analysis: paving the way to a diverse library for glycobiologists, Chem. Sci. 8 (12) (2017) 7932–7940.
[23] R. Novoa-Carballal, A.H.E. Müller, Synthesis of polysaccharide-b-PEG block copolymers by oxime click, Chem. Commun. 48 (31) (2012) 3781–3783.
[24] R. Novoa-Carballal, C. Silva, S. Moller, M. Schnabelrauch, R.L. Reis, I. Pashkuleva, Tunable nano-carriers from clicked glycosaminoglycan block copolymers, J. Mater. Chem. B 2 (26) (2014) 4177–4184.
[25] C.D. Sommers, H. Ye, J. Liu, R.J. Linhardt, D.A. Keire, Heparin and homogeneous model heparin oligosaccharides form distinct complexes with protamine: light scattering and zeta potential analysis, J. Pharm. Biomed. Anal. 140 (2017) 113–121.
[26] Á. Piñeiro, E. Muñoz, J. Sabín, M. Costas, M. Bastos, A. Velázquez-Campoy, P. F. Garrido, P. Dumas, E. Ennifar, L. García-Río, J. Rial, D. Pérez, P. Fraga, A. Rodríguez, C. Cotelo, AFFINImeter: a software to analyze molecular recognition processes from experimental data, Anal. Biochem. 577 (2019) 117–134.
[27] E. Muñoz, J. Sabín, The use of ITC and the software AFFINImeter for the quantification of the anticoagulant Pentasaccharide in low molecular weight heparin, in: E. Ennifar (Ed.), Microcalorimetry of Biological Molecules: Methods and Protocols, Springer New York, New York, NY, 2019, pp. 215–223.
[28] G. Pasut, F.M. Veronese, State of the art in PEGylation: the great versatility achieved after forty years of research, J. Control. Release 161 (2) (2012) 461–472.
[29] R. Novoa-Carballal, A.H.E. Muller, Synthesis of polysaccharide-b-PEG block copolymers by oxime click, Chem. Commun. 48 (31) (2012) 3781–3783.
[30] R. Novoa-Carballal, C. Silva, S. Moller, M. Schnabelrauch, R.L. Reis, I. Pashkuleva, Tunable nano-carriers from clicked glycosaminoglycan block copolymers, J. Mater. Chem. B 2 (26) (2014) 4177–4184.
[31] D. Thakar, E. Migliorini, L. Coche-Guerente, R. Sadir, H. Lortat-Jacob, D. Boturyn, O. Renaudet, P. Labbe, R.P. Richter, A quartz crystal microbalance method to study the terminal functionalization of glycosaminoglycans, Chem. Commun. 50 (96) (2014) 15148–15151.
[32] E.M. Muñoz, R.J. Linhardt, Heparin-binding domains in vascular biology, Arterioscler. Thromb. Vasc. Biol. 24 (9) (2004) 1549–1557.
[33] R. Novoa-Carballal, D.V. Pergushov, A.H.E. Muller, Interpolyelectrolyte complexes based on hyaluronic acid-block-poly(ethylene glycol) and poly-l-lysine, Soft Matter 9 (16) (2013) 4297–4303.
[34] S.M. Bromfield, P. Posocco, M. Fermeglia, S. Pricl, J. Rodriguez-Lopez, D.K. Smith, A simple new competition assay for heparin binding in serum applied to multivalent PAMAM dendrimers, Chem. Commun. 49 (42) (2013) 4830–4832.
[35] V.A. Kabanov, Polyelectrolyte complexes in solution and in bulk, Russ. Chem. Rev. 74 (1) (2005) 3–20.
[36] J. Hirsh, S.S. Anand, J.L. Halperin, V. Fuster, Guide to anticoagulant therapy: heparin, Circulation 103 (24) (2001) 2994–3018.
[37] L. Ma, J. Huang, X. Zhu, B. Zhu, L. Wang, W. Zhao, L. Qiu, B. Song, C. Zhao, F. Yan, In vitro and in vivo anticoagulant activity of heparin-like biomacromolecules and the mechanism analysis for heparin-mimicking activity, Int. J. Biol. Macromol. 122 (2019) 784–792.
[38] F.M. Veronese, G. Pasut, PEGylation, successful approach to drug delivery, Drug Discov. Today 10 (21) (2005) 1451–1458.